Universiteit Leiden
The Netherlands

Omic-scale high-throughput quantitative LC-MS/MS approach for circulatory lipid phenotyping in clinical research

Medina, J.; Borreggine, R.; Teav, T.; Gao, L.; Ji, S.S.; Carrard, J.; ... ; Ivanisevic, J.

Note: To cite this publication please use the final published version (if applicable).

Omic-Scale High-Throughput Quantitative LC−MS/MS Approach for Circulatory Lipid Phenotyping in Clinical Research

Jessica Medina, Rebecca Borreggine, Tony Teav, Liang Gao, Shanshan Ji, Justin Carrard, Christina Jones, Niek Blomberg, Martin Jech, Alan Atkins, Claudia Martins, Arno Schmidt-Trucksass, Martin Giera, Amaury Cazenave-Gassiot, Hector Gallart-Ayala,* and Julijana Ivanisevic*
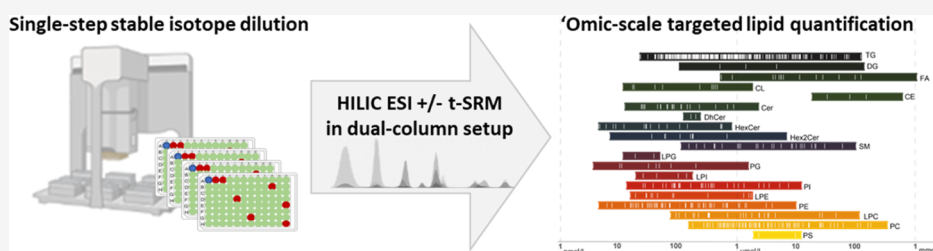
ACCESS | Metrics & More | Article Recommendations | SI Supporting Information

ABSTRACT: Lipid analysis at the molecular species level represents a valuable opportunity for clinical applications due to the essential roles that lipids play in metabolic health. However, a comprehensive and high-throughput lipid profiling remains challenging given the lipid structural complexity and exceptional diversity. Herein, we present an 'omic-scale targeted LC−MS/MS approach for the straightforward and high-throughput quantification of a broad panel of complex lipid species across 26 lipid (sub)classes. The workflow involves an automated single-step extraction with 2-propanol, followed by lipid analysis using hydrophilic interaction liquid chromatography in a dual-column setup coupled to tandem mass spectrometry with data acquisition in the timed-selective reaction monitoring mode (12 min total run time). The analysis pipeline consists of an initial screen of 1903 lipid species, followed by high-throughput quantification of robustly detected species. Lipid quantification is achieved by a single-point calibration with 75 isotopically labeled standards representative of different lipid classes, covering lipid species with diverse acyl/alkyl chain lengths and unsaturation degrees. When applied to human plasma, 795 lipid species were measured with median intra- and inter-day precisions of 8.5 and 10.9%, respectively, evaluated within a single and across multiple batches. The concentration ranges measured in NIST plasma were in accordance with the consensus intervals determined in previous ring-trials. Finally, to benchmark our workflow, we characterized NIST plasma materials with different clinical and ethnic backgrounds and analyzed a sub-set of sera ($n = 81$) from a clinically healthy elderly population. Our quantitative lipidomic platform allowed for a clear distinction between different NIST materials and revealed the sex-specificity of the serum lipidome, highlighting numerous statistically significant sex differences.

INTRODUCTION

The lipidome comprises a large set of lipid-like metabolites with diverse chemical properties and biological roles, including cell membrane constituents, energy storage, and signaling molecules. Given these key roles that lipids play in cellular metabolism, significant efforts toward systematic characterization of lipidome composition are ongoing in a wide range of biological samples.[1−3] In human plasma, around 700 lipid species were annotated in the last decade,[4] representing approximately 70% of the whole plasma metabolome in terms of species diversity as well as relative abundance.[3,5] Among diverse circulatory lipids, complex lipids constitute 60% of the total lipidome. Complex lipids owe their name to representative building blocks: a glycerol backbone, a polar head group, fatty acyl/alkyl chains that vary in length and number of unsaturated carbons, or a sterol ring structure. They encompass diverse lipid classes such as glycerolipids (GLs),

glycerophospholipids (GPs), sphingolipids (SPs), and sterol lipids including cholesteryl esters (CEs).[6]

The interest in a comprehensive measurement of the human plasma lipidome has increased due to the physiological and clinical relevance of lipid profiles.[1,7,8] In routine clinical assays, lipids are generally measured as the total content of triglycerides and of cholesterol, employed as main predictors of cardiovascular events.[9] However, cardiometabolic risk assessment based on these parameters lacks specificity for diagnostics and sensitivity for early prediction of disease
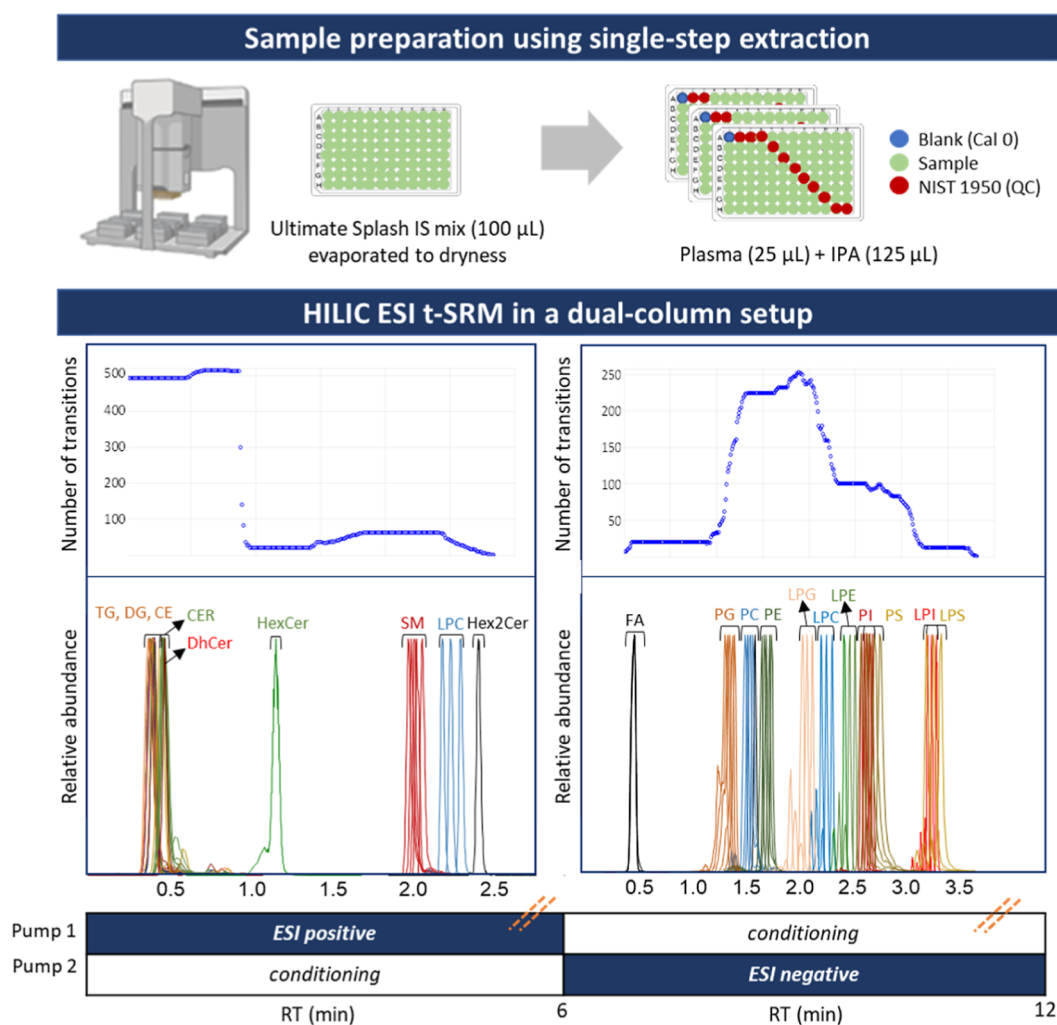
Figure 1. Workflow of semi-automated sample preparation and HILIC−MS/MS analysis in the SRM mode. (A) Samples are prepared on the automated liquid-handling platform using a 96-well plate format. First, a mixture of internal standards is added to each well, followed by evaporation to dryness. Then, the dried IS extracts are reconstituted with the plasma matrix (25 μL) and IPA (125 μL) for lipid extraction (see the Experimental Section for details). The supernatants are collected and transferred to the injection plate. (B) Samples are analyzed using the HILIC−MS/MS approach in positive and negative ionization modes. Data acquisition is performed in the timed-selected reaction monitoring mode. Elution profile and transition distribution are given for the positive and negative ionization mode depending on lipid class. Lipid-class profiles are illustrated on the elution of deuterated internal standards representative of lipid classes (concerning the separation of species with differing acyl/alkyl-chain length and number of unsaturations, see Figure S1 for individual peak shape). The dual-pump setup allows for simultaneous conditioning of the first column, while the data are acquired on the second column, reducing the total run time to 12 min.

onset.[10] The acquisition of more comprehensive and specific circulatory lipid signatures could significantly improve the sensitivity and accuracy of clinical prognosis and diagnosis of cardiometabolic outcomes in a sex-stratified manner.[11−13] Moreover, association analyses between concentrations of specific lipids and cardiometabolic risk factors (e.g., age, sex, BMI—body mass index, WHR—waist-to-hip ratio, hormonal transitions, hypertension, and dyslipidemia) and health outcomes (e.g., obesity, diabetes, and cardiovascular diseases) will improve our understanding of lipid roles in disease etiology.

The translation of lipid profiling to clinical laboratories is still hindered by the lack of the necessary amount of cross-comparable quantitative lipid data acquired on different populations worldwide.[14,15] However, the fundamental efforts to establish analytical consensus values in reference materials (e.g., NIST SRM 1950 plasma) and investigate strategies for data harmonization have already been made by the lipidomics community (http://lipidomics-standards-initiative.org).[3,16−20] The systematic analysis of shared reference materials has emerged as the best normalization strategy to correct method-specific biases (e.g., application of different extraction procedures and analytical platforms for lipid measurement).[21−25] Thus, the time is right to foresee the collection of biologically relevant data necessary to establish the reference intervals for populations with different ethnic backgrounds and dietary regimens across different geographical regions.

Advancements in mass spectrometry (MS) technology have improved the sensitivity and selectivity of lipid analysis allowing for the measurement of several hundred lipid species from minimal sample amount in a high-throughput manner.[26−28] The most commonly used MS-based approaches for comprehensive lipid analysis at large-scale (i.e., clinical research) still consist of direct infusion MS techniques (DIMS) using either intra-source[29−31] or ion mobility separation (Lipidyzer platform).[32−34] The main drawback of

DIMS is the ion suppression and the lack of sensitivity for the quantification of low abundant species.[26−35] Therefore, hyphenated techniques with higher separation capacity, such as liquid chromatography (LC) and supercritical fluid chromatography coupled to MS, have recently gained significant interest.[36] They represent an alternative for the analysis of low abundant lipids and isobaric species, thus offering the widest coverage.[37,38] Lipid analysis using LC−MS can be addressed by reversed-phase LC (RPLC),[4,39] where lipid species are separated according to the hydrophobicity of the acyl-chains, or hydrophilic interaction liquid chromatography (HILIC),[40,41] where lipids are separated based on their polar head groups resulting in lipid-class separation.

The accuracy and robustness of lipid quantification depend, among other factors, on the comprehensiveness of the internal standard (IS) panel. In RPLC, an extensive IS panel is required to correct for matrix effects due to lipid species separation according to the acyl-chain composition. The elution of endogenous species and surrogate IS in varying solvent compositions represents an important challenge for the appropriate correction of matrix effects. Recently, an innovative approach using ^{13}C labeled yeast extract (LILY) has been proposed by Rampler et al.[42] to quantify 350 lipid species from seven lipid classes. However, the pitfall of this approach constitutes the evaluation of the labeled lipid concentrations in each batch of yeast extract prior to its application. While RPLC offers high chromatographic resolution for a more comprehensive qualitative lipid characterization,[4] HILIC-based approaches facilitate the development of quantitative methods because endogenous lipids follow class separation and co-elute with their corresponding internal standards in the same solvent composition.[39,43] Therefore, fewer internal standards are required to correct matrix effects.[39] Still, it remains essential that the IS mixture contains multiple representatives of each lipid class with varied fatty acid compositions to correct the differential ionization and fragmentation efficiencies depending on the fatty acid chain length and degree of unsaturation.[44]

This work aimed to develop a maximum-coverage and high-throughput targeted HILIC−MS/MS workflow for the robust quantification of lipids in human plasma and other complex biological matrices. The method precision was evaluated through intra- and inter-day analysis of independently extracted pooled plasma samples and NIST reference material as quality control (QC). Lipid concentration ranges were measured in different NIST plasma reference materials (SRM 1950, diabetic—T1D, high triglyceride—h-TG, young African—American—YAA) and cross-evaluated against previous inter-laboratory studies.[18] Finally, the established HILIC−MS/MS method was applied to a sub-group of clinically healthy, aged participants from the COmPLETE-Health study to elucidate sex differences across human lipid profiles.

■ EXPERIMENTAL SECTION

Chemicals and Reagents and Internal Standard Mixture Preparation. Chemicals and reagents and internal standard mixture preparation (see Table S1) are described in the Supporting Information.

COmPLETE-Health Study. A subset of clinically healthy age- and sex-balanced participants [n = 81, 42 males aged 73.50 ± 4.06 and 39 females aged 74.33 ± 2.90, p-value (age) = 0.4280] from the COmPLETE-Health cohort (https://www.complete-project.ch/)[45] were selected for the investigation of

sex differences across plasma lipidome. Clinical characteristics of the selected healthy sub-cohort are reported in Table S2.

Semi-Automated Sample Preparation Using a Liquid Handling Platform. The IS mixture (100 μL) was added to 2 mL 96-deepwell (Waters, Milford, MA, USA) plates using a Bravo automated liquid-handling platform (Agilent Technologies, Santa Clara, California, USA), following the evaporation to dryness in a vacuum concentrator (TurboVap 96, Biotage, Charlotte, NC, United States) (Figure 1). The dried IS mixture was reconstituted by adding 25 μL of plasma sample and mixed on a shaker for 3.5 min to allow for the interaction. Finally, 125 μL of IPA was added for lipid extraction and protein precipitation using the Bravo system. Extracts were shaken (10 min at 1000 rpm) and centrifuged externally (15 min at 20,000g at 20 °C) (Hermle Z 326 K, Gosheim, Germany). Finally, the supernatant (75 μL) was transferred, using the liquid handler, to a new 96-well plate (Thermo Scientific, San Jose, CA, United States) for LC−MS/MS analysis.

LC−MS/MS Analysis. The plasma extracts were analyzed by HILIC−MS/MS using a dual-column setup coupled to tandem MS. Analysis was performed on a Vanquish Duo UHPLC system coupled to a TSQ Altis triple-stage quadrupole mass spectrometer (Thermo Scientific, San Jose, CA, United States) in positive and negative ionization modes. The chromatographic separation, as described previously,[46] was carried out on an Acquity Premier BEH Amide column (1.7 μm, 100 mm × 2.1 mm I.D., Waters, Milford, MA, USA). A dual-column setup allowed for the re-equilibration of the first column while analyzing the sample on a second column, thus significantly reducing the total analysis time per sample. Analytical conditions and MS parameters are described in the Supporting Information. Selected reaction monitoring (SRM) transitions are provided in Tables S3−S5. Fragmentation patterns and structural annotation is shown on Scheme S1. Lipid nomenclature and data processing and statistical analyses are provided in the Experimental Section of the Supporting Information.

Linearity Assessment in Plasma Matrix. To evaluate the linearity of the lipid response in a complex plasma matrix, the UltimateSPLASH ONE internal standard mixture (see concentrations per species in Table S1) was diluted (1/20) (v/v) with IPA. Different volumes of the diluted mixture (2, 5, 10, 20, 30, 50, 60, 100, 500, 1000, 1500, and 1750 μL) (Table S8) were distributed to Eppendorf tubes and evaporated to dryness in a vacuum concentrator (LabConco, Kansas City, MO) (Figure S2) followed by the reconstitution with 25 μL of NIST plasma SRM 1950 and 125 μL of isopropanol (IPA) for lipid extraction.

Repeatability Assessment. A total of 252 independently extracted pooled plasma samples were analyzed together with NIST SRM 1950 plasma as QC across three 96-well plates and over 3 different days (Table S9). Each batch comprised blanks, 84 plasma samples, and 11 NIST SRM 1950 (injected every 12 samples). The intra- and inter-day precision were evaluated by the coefficient of variation (CV) calculated on lipid concentrations from QC NIST plasma across one and three batches of analysis, respectively (Figure 3 and Table S9).

Isotopic Overlap Correction. The contribution of heavy isotopes to the SRM transition intensities depends on their location in the molecule with respect to the fragmentation pattern.[47] Correction for isotopic overlap based on lipid class separation by SRM was performed using the Shiny app of
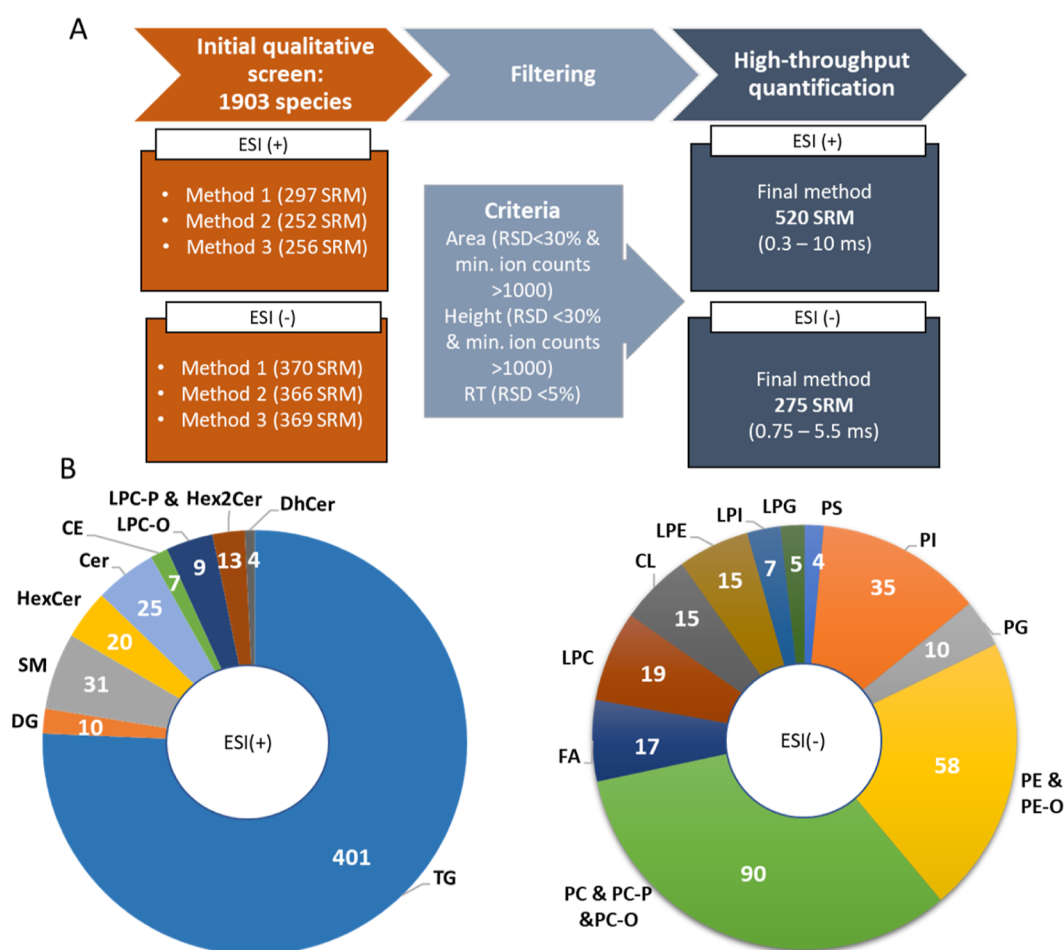
Figure 2. Analytical workflow for human plasma samples: from initial qualitative screening to high-throughput quantification. (A) An initial qualitative screen targets 1903 lipids in NIST plasma reference material [ESI(+) 798 SRM and ESI(−) 1105 SRM] (Tables S3−S5). To successfully englobe this extensive targeted list, transitions were distributed across three independent SRM methods per ionization mode. Acquired data were filtered based on the RSD of peak area, height, and retention time. The final quantitative method included 795 detectable lipid species [ESI(+) 520 SRM and ESI(−) 275 SRM] (Table S6). (B) Coverage of detectable plasma lipidome per lipid class. Of note, lipids quantified with the final method are still subject to drift correction and measurement precision evaluation (see the Measurement Precision section and Figure 3).

LICAR (https://slinghub.shinyapps.io/LICAR/) developed by Gao et al.[47]

RESULTS AND DISCUSSION

A high-throughput quantitative HILIC−MS/MS approach was developed to perform large-scale lipid screening and quantification using SRM. Importantly, HILIC analysis allows for lipid class separation according to polar headgroups as shown on the internal standard mixture profile in Figure 1. Lipid class separation facilitates the development of quantitative methods due to the coelution of endogenous species with IS. Thereby, the appropriate correction of matrix effects is accomplished by the corresponding IS eluting in the same solvent and matrix composition.[39]

From Semi-Automated Sample Preparation to High-Throughput HILIC−MS/MS Analysis. Single-step lipid extraction using 2-propanol (IPA)[46,48] was automated for 96-well plate formats using a liquid-handling platform (Figure 1), thus maximizing the reproducibility and efficiency of sample preparation.[49,50] Sample analysis was then carried out by HILIC as described above. In positive ionization, 11 lipid sub-classes are analyzed (for lipid nomenclature see the Supporting Information), eluting as follows: neutral lipids including DG,

TG, and CE, followed by Cer, DhCer, HexCer, SM, ether-linked LPC (including plasmalogens), and Hex2Cer and Hex3Cer. In negative ionization, 15 sub-classes are targeted in the following elution order: FA, PG, PC, PE, CL, and corresponding lysophospholipids (LP) including LPG, LPC, and LPE, followed by PS and PI, and finally LPI and LPS (Figure 1). Importantly, MG was not included due to lack of selectivity (i.e., low fragmentation efficiency). Moreover, high-resolution mass spectrometry analyses imply that the signal corresponding to MG likely represents an interference from the background chemical noise (and not a consequence of in-source fragmentation of DG or TG). This was further supported by some plasticizer, poly(ethylene glycol), and Triton surfactant matches against MaConDa (https://www.maconda.bham.ac.uk/). The selectivity needed for lipid annotation is defined by fragmentation patterns: headgroup-based transition for SM, fatty acid neutral losses for GL, long-chain sphingoid bases (LCB) for Cer, and fatty acyl/alkyl-chain-based transitions for GP, as listed in Scheme S1. In negative ionization, the GP profile is obtained according to their headgroups. Furthermore, the SRM allows for the characterization of the acyl- or alkyl-chain composition,[51] which constitutes valuable information for biological inter-
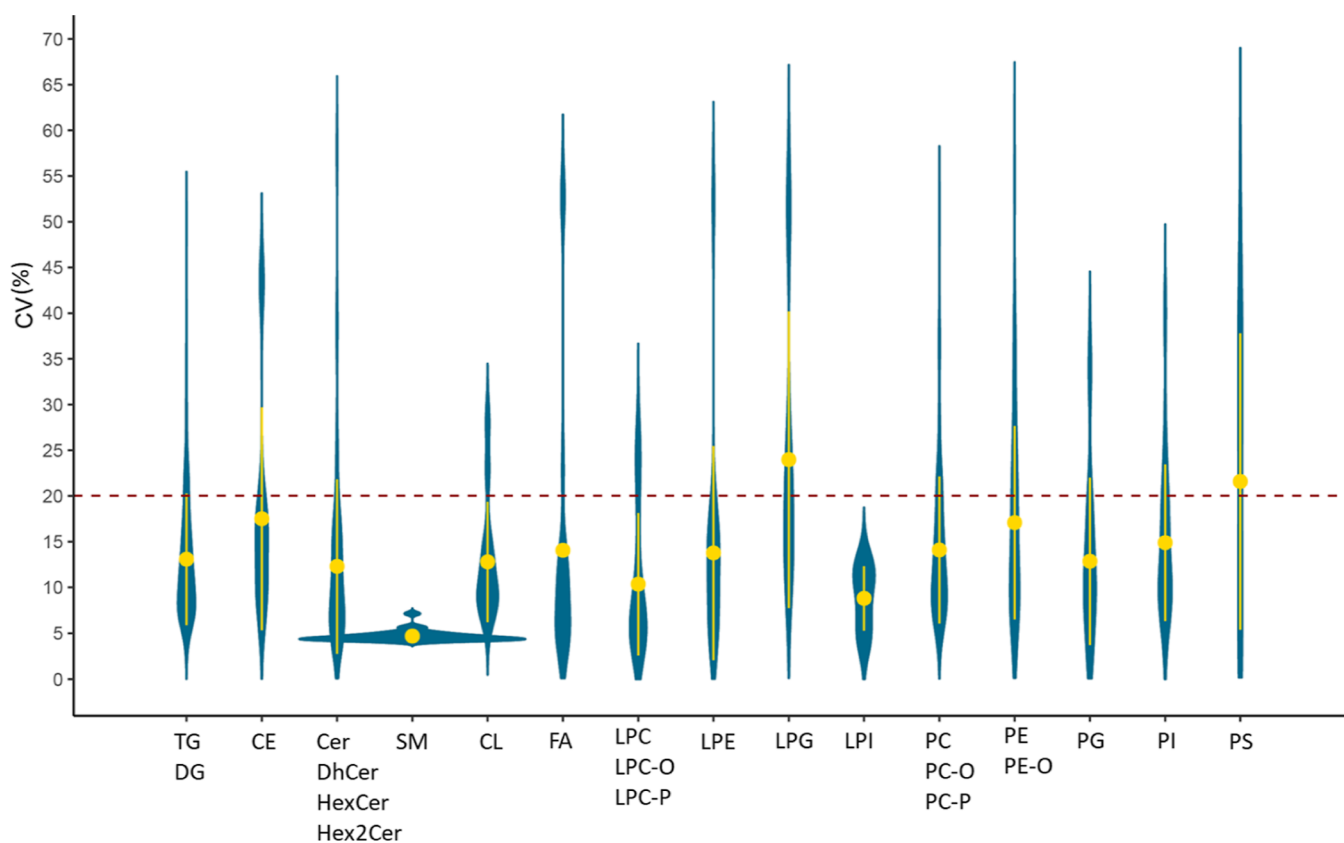
Figure 3. Inter-day measurement precision per lipid class. Method repeatability was determined by analyzing three 96-well plates of independently extracted pooled plasma samples and NIST reference material (as QC) across several days. Distribution of coefficients of variation for each lipid class is presented by respective violin plots. The yellow dot and line represent mean and SD. Reproducibility data per lipid species and lipid class are given in Tables S9 and S10.

pretations. As a result of neutral loss, the fatty acid composition can also be determined for DG and CE, while for TG, the composition of only one acyl chain can be deduced. The targeted lists of corresponding SRM transitions are provided in Tables S3−S6. One drawback of the described HILIC setting is the poor retention of neutral lipids due to the absence of polar functional groups. However, despite significant co-elution in specific areas of the chromatographic gradient, reliable peak definition is maintained owing to the unprecedented acquisition rate of the instrument (down to 0.25 ms of dwell time) (Figure S1). This enables the acquisition of a minimum of 8−10 scans per peak, even in the areas where several hundred species are co-eluting (i.e., in the void volume in positive ionization mode). In other areas, along with the gradient, dwell time is maintained from 0.7 to 10 ms depending on the number of targeted species (Tables S3−S6).

To maximize the lipid coverage, the HILIC−MS/MS analysis pipeline was designed in two steps: (1) initial screen of an extensive lipid panel followed by (2) filtering of chemical/informatic noise (based on signal reproducibility as indicated below) and (3) high-throughput quantification of filtered, robustly detectable lipid species, as shown for plasma in Figure 2A. With respect to the applied workflow, we report the lipidome coverage as follows: (1) species targeted by the initial screen, (2) detected in human plasma, and (3) quantified in human plasma (with CV < 20%) (Table S7). The initial screen is performed on pooled samples, representative of the entire sample batch, and currently

comprises 1903 theoretical targets, which can be further extended. This comprehensive targeted list was assembled based on commonly reported and recently characterized lipid species in human plasma, serum, whole blood, and different types of blood cells.[4,34,52] With this initial screen, 817 lipid species are targeted in positive and 1105 species in the negative ionization mode, with the equivalent number of transitions (SRM) (Tables S3−S6) distributed across three independent methods per ionization mode (Figure 2). Because the instrument acquisition rate represents a limiting factor when targeting several hundred transitions, applying multiple methods increases the sensitivity and data quality for the qualitative characterization of the detectable lipidome before high-throughput quantification. Following the initial qualitative screen, detectable lipid species are filtered using the following criteria across five consecutive injections of pooled samples: relative standard deviation (RSD) of retention time (RSD < 5%), peak area (min. ion counts > 1000, and RSD < 30%), height (min. ion counts > 1000 and RSD < 30%), and lipid presence in at least 80% of replicates. Lipid species that pass these quality filters are merged into a final targeted list for high-throughput quantification. For human plasma, based on the initial screen of NIST reference material, 795 lipid species [520 SRM in ESI(+) and 275 SRM in ESI(−), Figure 2A] were retained for quantification and analyzed in a 12 min total time. These 795 detected lipid species span 24 different lipid sub-classes, including 411 GL (DG, TG), 212 GP (PC, PE, PG, PI, PS, and CL), 93 SP (Cer, DhCer, HexCer, Hex2Cer, and SM), 55 LP (LPE, LPC, LPI, and LPG), 17 FA, and 7 CE (Figure
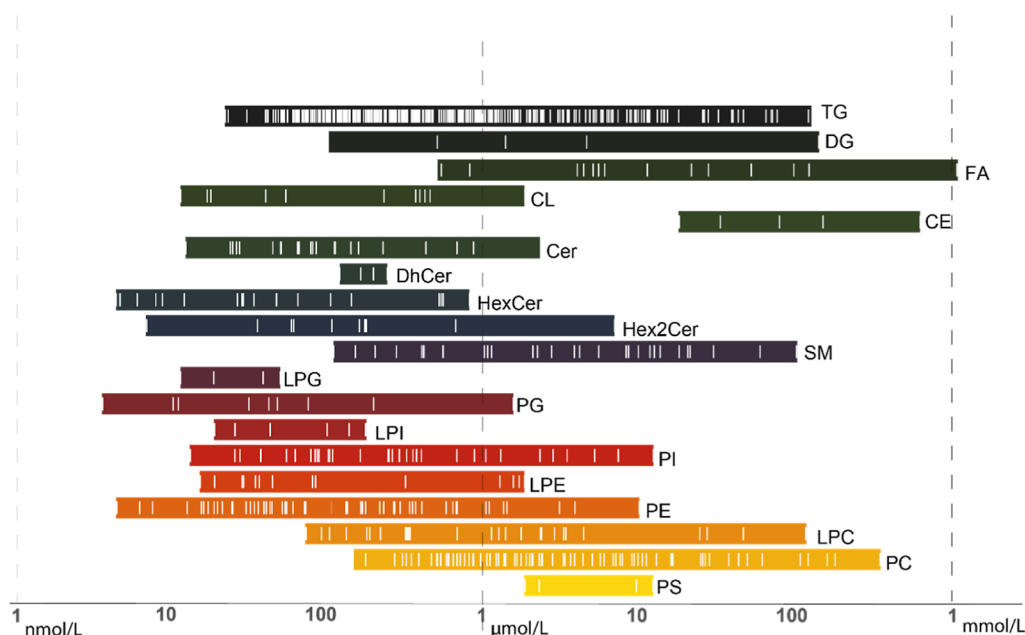
Figure 4. Concentration ranges of lipids measured by the presented HILIC−MS/MS method in NIST SRM 1950 plasma. Vertical white lines represent the measured concentrations of different lipid species in their corresponding class. Data were normalized using log transformation and molar concentrations were back calculated for ease of interpretation (see Table S13).

2B). This comprehensive lipid screen allows for the broadest coverage of lipid classes comprising a wide diversity of lipid species with high annotation specificity. Of 795 detected species, 377 were characterized at the level of acyl chain identity, 401 TG with the composition of one acyl chain, and 31 SM at the level of acyl chain sum composition. Importantly, the presented HILIC approach offers the extended coverage of SP and GP species (along with ether-linked species, PI, PS, LPS, and LPS). For comparison, the commonly applied DIMS quantification method using Lipidyzer[18] and one of the most comprehensive RPLC-based approaches[4] allow for detecting 737 and 636 unique lipid species in human plasma, respectively. In general, the coverage is dependent on the sample type and its composition.[53]

Linearity Assessment. Lipid quantification represents a challenge given the wide concentration ranges in which they can be present in biological matrices, spanning 9 orders of magnitude.[15] Even within the single class, different lipid species can span more than 4 orders of concentrations, like TG, for example. To quantify this large diversity of lipid species spanning wide concentration ranges, we opted for a single-point calibration, a widely used alternative strategy in the lipidomics field.[29,54] This approach considers the steady response factors within the same matrix and allows us to estimate the concentration of an analyte with respect to the IS spike at a known concentration.[55] Before applying the single-point calibration for concentration estimation, we evaluated the linearity of our method for different lipid classes in the NIST plasma matrix using the UltimateSPLASH IS mixture (Avanti Polar Lipids) (Figure S2). The calibration curves of the entire IS panel representative of different lipid classes were found to be linear ($R^2 > 0.97$, except for one CE and two DG) over a broad concentration range (Table S8 and Figure S2) in which different classes were previously reported in human plasma (e.g., consensus intervals[17]). Based on the linearity assessment, we deduced the most suitable concentration for the IS mixture spike to the plasma matrix to quantify the entire

panel of lipid species using single-point calibration (Table S1). The assignment of surrogate IS was made depending on the lipid class and the most similar acyl/alkyl chain composition (based on chain length and number of unsaturations—see Tables S3 and S4). Similar strategies are applied in shotgun,[29] RPLC-based targeted,[56] and untargeted lipidomic assays.[40]

Measurement Precision. Repeatability of the final quantitative method (including 795 lipids detected in human plasma) was evaluated by intra- and inter-day analysis of independently extracted plasma samples with NIST reference material as QC, injected periodically every 12 samples. NIST reference material has become a prerequisite for large-scale studies; its function can be twofold: (1) to serve as a QC to correct for within and between batch signal intensity drift (as alternative to a representative pool of thousands of participants in a population study) and (2) to allow for cross-comparison of data acquired by different methodologies.[15,57] We used the LOWESS method (span = 0.9) to correct the signal intensity drift over time based on the response of lipid species detected in the NIST plasma used as a QC (Figure 3).

Following the signal intensity drift correction, 716 were measured with intra-day repeatability <20%, whereas the inter-day variability <20% was achieved for 661 species (or 85%) present in human plasma (Tables S9 and S10). Lipid species with poor retention and ionization efficiency, such as CE, showed the highest signal variability in intra- and inter-day experiments (Figure 3). This was also true for low abundant species, such as DG, LPG, and PS. As specified above, the extensive coverage of our method is in accordance with the results reported with the Lipidyzer kit, where 704 lipid species belonging to 13 major lipid classes, among which more than 70% TG, were measured with high reproducibility (CV < 20%) in human plasma.[18] Using the presented HILIC approach, the coverage of SP and PL was significantly extended to encompass more than 50% of quantified lipid species and overall, 24 different lipid subclasses (Table S7) in human plasma.
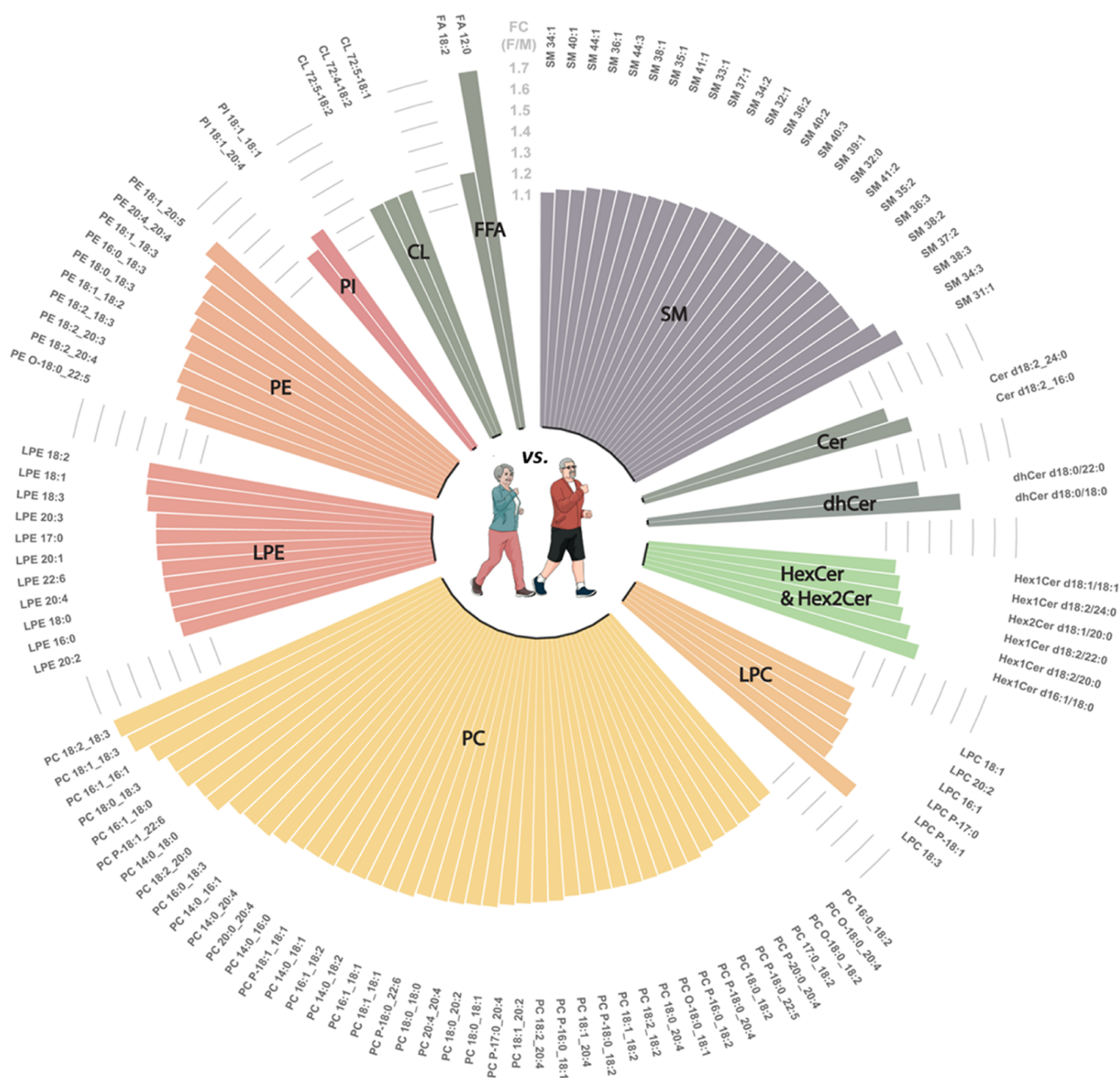
Figure 5. Sex differences across human lipidome were revealed in a sub-group of clinically healthy elderly participants from the COmPLETE Health cohort (www.complete-project.ch). A circular barplot organized per lipid class highlights lipid species displaying significantly higher levels in females compared to males (F vs M, adjusted *p*-value ≤ 0.05). Bar plots represent the female to male concentration ratio.

Correction of Isotopic Overlap. Lipid class separation in HILIC has the drawback of isotopic overlap where M + 2 isotopologue of co-eluting lipid species with one additional unsaturation will interfere with monoisotopic *m/z* of species with one unsaturation less. Therefore, the isotopic correction was performed using the LICAR application specifically developed for SRM or MRM data to avoid introducing an additional bias to lipid quantification. The calculation of heavy isotope contribution depends on the lipid fragmentation patterns.[47] The correction factor for the isotopic overlap is given in Table S11. Importantly, for some species, the isotopic interference was complete by the presence of significantly more abundant species with an additional unsaturation (see Table S11). It should be noted that the currently performed

correction is restricted to the targeted species and remains partial, specifically for diacyl species, due to inclusion of only one transition (corresponding to one fatty acyl chain). In MRM analysis, for diacyl species, each acyl tail combination can overlap with corresponding species with one more unsaturation and two heavy isotopes on the corresponding acyl tail and/or headgroup.[34] For complete correction of isotopic overlap among diacyl phospholipids, it is recommended to consider an additional list of transitions (which should be scanned in several additional runs during the initial screen) provided in Table S12. Depending on their presence in plasma or other sample type (determined during the initial screen), these transitions should be used to correct for the interference they might be causing.

Dynamic Range of Lipid Measurement in NIST Reference Material. Measured concentrations across different lipid classes spanned 6 orders of magnitude, with the highest concentrations reported for FA, CE, followed by PC, DG, and TG (Figure 4 and Table S13). TG spanned the broadest range of concentrations from low nM to high μM levels. Among the measured complex lipid species, specific HexCer, PG, and PE were found to be present at the lowest concentrations in human plasma. Also, in-line with earlier reports, LP was reported in lower concentrations than the corresponding GP.[14,17] Among high-coverage targeted approaches, the DIMS-based Lipidyzer platform was applied for lipid quantification in human cohort studies. Recently, a cross-laboratory comparison showed its excellent performance in terms of accuracy and precision.[18] Following this report, we compared the results obtained by our HILIC approach and the Lipidyzer platform. In terms of lipid coverage, the HILIC method allowed for quantifying a greater diversity of lipid species in human plasma (belonging to 24 different subclasses), mainly due to the added value of chromatographic separation for SP and PL. The overlap between both methods comprised 468 lipids (Table S14), including CE (5), Cer (6), DhCer (2), FA (13), HexCer (6), Hex2Cer (2), LPC (8), LPE (4), PC (24), PE (11), SM (12), and TG (375). Overall, the results show a high correlation between measured concentrations ($R^2 = 0.87$), except for CE and some FA (Figure S6). In general, the concentrations measured with the presented HILIC method were also consistent with the reported consensus values by the Bowden et al. ring trial.[17] The annotation at the sum composition level was used to allow for the comparison. The measured concentrations of overlapping species ($n = 174$, Table S15) showed high correlation ($R^2 > 0.78$) with some species-specific exceptions. These differences are likely related to different sample preparations and MS acquisition methods. It is also worth mentioning that in these previous studies the isotopic correction was not systematically performed. In addition, depending on the fatty acyl/alkyl composition of IS, the reported concentrations of symmetric versus asymmetric lipid species might be biased given the difference in intensity of product ions depending on the sn-position.[44] Finally, consensus values for DhCer, CL, and LPG remain to be established. In general, the correction of potential method-dependent discrepancies can be done based on the systematic analysis of NIST reference material in every sample batch to allow for data harmonization and cross-comparison.[14]

To further benchmark our method, we have characterized the additional NIST reference materials with different clinical and ethnic backgrounds (Table S16). The measured concentrations are provided in Table S13 and the differences in lipid composition are presented on Figures S3−S6. Important differences in the matrix effect were observed in different plasma samples depending on their lipid composition. These differences are reported in Table S17 and discussed in more details in the Supporting Information.

Sex Differences across Plasma Lipidome: COmPLETE-Health Cohort. As a proof of concept, to investigate the potential sex differences in plasma lipidome, we analyzed a subgroup ($n = 81$) of clinically healthy sex-balanced aged participants from the COmPLETE Health cohort (www.complete-project.ch) (see Table S2 for clinical characteristics and Table S18 for measured lipid concentrations). Using the established HILIC−MS/MS method, we were able to reveal numerous significant differences ($n = 112$, adjusted p-value <

0.05) in lipid levels between sexes (Figure 5). Interestingly, the entire panel of lipid species with varying concentrations showed 10 to 70% higher concentrations in females compared to males. This increase was observed primarily in two lipid classes: SP ($n = 35$ species), among which 25 SM, and GP ($n = 45$ species), represented mainly by PC and PE, including lysophospholipid species (Figure 5).

These results are in accordance with previous findings that demonstrated the sex-specificity of human plasma lipidome in several population studies, including AusDiab,[58] COmPLETE Health,[45] KORA,[59,60] GOLDN,[61] Healthy French,[62] and others.[63−65] They revealed multiple sex differences regardless of age and the sex-dependent age-related differences.[66] Specifically, the increased levels of SM and PC were positively associated with the female sex only.[45]

This significant difference related to SM was identified in women, starting from childhood.[67] There is no clear evidence about the origins of this difference; however, the hypothesis on the possible endocrine or sex-hormone driven modulation of the activity of enzymes involved in the synthesis and/or catabolism of sphingomyelins is plausible and was implied in previous studies that associated estradiol with sphingomyelin levels.[68,69] In addition, data suggest that SP themselves can also act as modulators of steroid hormone production.[70−72] Sphingomyelins play an important role in cell membrane formation and plasma lipoprotein metabolism comprising cholesterol efflux and cholesterol absorption, important sources for steroidogenesis. Finally, sphingomyelins and ceramides containing the d18:2 sphingadiene backbone were systematically found higher in females, which were associated with the higher activity of desaturase (FADS3) in females.[4,73] We could not confirm this directly because our method does not allow for the distinction between SP with d18:1 and d18:2 backbone (among others).

As stated previously, other major sex differences were observed in membrane lipids, PC, and PE.[28,59,74] PC are mainly located in the outer leaflet of plasma membranes. They are inherently linked to SP because they serve as a direct substrate for sphingomyelin synthesis via sphingomyelin synthases.[75] The sex bias found in PC and LPC levels might be explained by the reported difference in cholesterol acyltransferase (LCAT)[76] and phospholipase A2 (PLA2).[77] Previous studies have indeed demonstrated significantly lower PLA2 activity in women compared to men.[77] Finally, we also detected sex differences in ether-linked GP (PC-O and PC-P) with polyunsaturated (e.g., C20:4 and C18:2) fatty acid composition. These differences have also been highlighted in recent large-scale population studies, suggesting possible differences in female versus male dietary regimens and/or differential regulation of ether-phospholipid biosynthesis and degradation in the peroxisome, specifically with aging.[28,59,78,79]

In general, sex has been an overlooked variable in biomedical and clinical research; however, the awareness about important sex differences is growing, and multiple studies are ongoing in model systems and human populations to further explain the origins of these differences (e.g., hormonal status, environmental influences, microbiome, etc.)[71,80] and consider them in a more stratified and precise approach to medical care.

■ CONCLUSIONS

We present a high-coverage targeted HILIC−MS/MS lipidomics platform that measures over 1903 lipid species across 26 (sub)classes using a semi-automated sample

preparation workflow with single-step isopropanol extraction. When applied to human plasma reference material (NIST SRM 1950), the HILIC-based approach allows for the detection of 795 circulatory lipid species, of which 85% were quantified with high repeatability (< 20%) across multiple batches. Importantly, the approach uses the commercially available UltimateSPLASH mixture of isotopically labeled standards (which can be further complemented as described) with multiple representatives of each lipid class with varied acyl/alkyl chain composition and unsaturation degree. In a dual-column setup, the total analysis time is kept to 12 min (positive and negative ionization modes combined). In analogy to untargeted approaches, the within- and between-batch correction was achieved by the analysis of NIST reference material 1950 periodically within each batch of samples. The analysis of reference material(s) has emerged as the best strategy for data harmonization across multiple studies and laboratories. It should be noted that the presented method is an alternative for global analysis (in a straightforward way) and the limitations related to the measurement of specific classes (e.g., low abundant DG and poorly ionizable CE) should be considered. If one's research question focuses on DG or CE, an optimized method for these classes should be used.

The presented HILIC–MS/MS approach was benchmarked on a subgroup of participants from COmPLETE Health cohort (www.complete-project.ch). It enabled the identification and quantification of numerous subtle (10−70%) but statistically significant sex differences across circulatory lipids. This study demonstrates the value of quantitative analysis to reveal small but physiologically relevant changes and warrants the application of the presented targeted lipidomics platform in biomedical and clinical research studies.

■ ASSOCIATED CONTENT

ⓈI Supporting Information

The Supporting Information is available free of charge at https://pubs.acs.org/doi/10.1021/acs.analchem.2c02598.

Preparation of internal standard mixture, clinical characteristics of the COmPLETE cohort, SRM list of lipid species in ESI(+), SRM list of lipid species in ESI(−), SRM list of internal standards in ESI(+) and ESI(−), SRM list of lipids detected in ESI(+) and ESI(−), lipid coverage results of the linearity assessment, results for the intra- and inter-day analyses, coefficients of variations per lipid class, isotopic correction factors per lipid species, SRM library of transitions corresponding to diacyl phospholipids which could interfere with species targeted in initial screen (with respect to targeted fatty acyl chain) and cause the isotopic overlap, estimated concentrations for NIST materials, lipid species detected by both Lipidyzer and HILIC–MS/MS, lipid species detected by HILIC–MS/MS and reported in ring-trial by Bowden et al., metadata for the NIST materials, evaluation of matrix effects in different plasma samples, and lipids detected in the samples of human sera collected from the participants of COmPLETE cohort (XLSX)

Lipidyzer sample preparation protocol, fragmentation patterns per lipid class, peak definition for representative lipid classes in the HILIC–MS/MS, workflow for linearity assessment, PCA plot for lipid profiles obtained for the different reference materials, circular barplot

displaying lipid species whose levels vary significantly in patients with hypertriglyceridemia compared to NIST SRM 1950, circular barplot displaying significant differences in lipid levels between NIST material collected from young African Americans and NIST SRM 1950, circular barplot displaying significant differences in lipid levels in patients with confirmed diabetes (T1D) compared to NIST SRM 1950, and cross-correlation of lipid concentrations quantified by the HILIC−MS/MS method and DIA using Lipidyzer (PDF)

■ AUTHOR INFORMATION

Corresponding Authors

Hector Gallart-Ayala − *Metabolomics Platform, Faculty of Biology and Medicine, University of Lausanne, Lausanne CH-1005, Switzerland*; Email: hector.gallartayala@unil.ch

Julijana Ivanisevic − *Metabolomics Platform, Faculty of Biology and Medicine, University of Lausanne, Lausanne CH-1005, Switzerland*; ⓘ orcid.org/0000-0001-8267-2705; Email: julijana.ivanisevic@unil.ch

Authors

Jessica Medina − *Metabolomics Platform, Faculty of Biology and Medicine, University of Lausanne, Lausanne CH-1005, Switzerland*

Rebecca Borreggine − *Metabolomics Platform, Faculty of Biology and Medicine, University of Lausanne, Lausanne CH-1005, Switzerland*

Tony Teav − *Metabolomics Platform, Faculty of Biology and Medicine, University of Lausanne, Lausanne CH-1005, Switzerland*

Liang Gao − *Department of Biochemistry and Precision Medicine TRP, Yong Loo Lin School of Medicine and Singapore Lipidomics Incubator, Life Sciences Institute, National University of Singapore, Singapore 117456, Singapore*; ⓘ orcid.org/0000-0003-3700-1069

Shanshan Ji − *Singapore Lipidomics Incubator, Life Sciences Institute, National University of Singapore, Singapore 117456, Singapore*

Justin Carrard − *Division of Sports and Exercise Medicine, Department of Sport, Exercise and Health, University of Basel, Basel CH-4052, Switzerland*; ⓘ orcid.org/0000-0002-2380-105X

Christina Jones − *Material Measurement Laboratory, National Institute of Standards and Technology, Gaithersburg, Maryland 20899, United States*; ⓘ orcid.org/0000-0001-7571-3062

Niek Blomberg − *Center for Proteomics and Metabolomics, Leiden University Medical Center, Leiden 2333ZA, Netherlands*

Martin Jech − *Thermo Fisher Scientific, San Jose, California 95134, United States*

Alan Atkins − *Thermo Fisher Scientific, San Jose, California 95134, United States*

Claudia Martins − *Thermo Fisher Scientific, San Jose, California 95134, United States*

Arno Schmidt-Trucksäss − *Division of Sports and Exercise Medicine, Department of Sport, Exercise and Health, University of Basel, Basel CH-4052, Switzerland*

Martin Giera − *Center for Proteomics and Metabolomics, Leiden University Medical Center, Leiden 2333ZA, Netherlands*; ⓘ orcid.org/0000-0003-1684-1894

Amaury Cazenave-Gassiot — *Department of Biochemistry and Precision Medicine TRP, Yong Loo Lin School of Medicine and Singapore Lipidomics Incubator, Life Sciences Institute, National University of Singapore, Singapore 117456, Singapore;* orcid.org/0000-0002-3050-634X

Complete contact information is available at:
https://pubs.acs.org/10.1021/acs.analchem.2c02598

Author Contributions

The manuscript was written through contributions of all authors. All authors have given approval to the final version of the manuscript.

Notes

The authors declare no competing financial interest.

■ REFERENCES

(1) Lange, M.; Angelidou, G.; Ni, Z.; Criscuolo, A.; Schiller, J.; Blüher, M.; Fedorova, M. *Cell Rep. Med.* **2021**, *2*, 100407.

(2) Muralidharan, S.; Shimobayashi, M.; Ji, S.; Burla, B.; Hall, M. N.; Wenk, M. R.; Torta, F. *Cell Rep.* **2021**, *35*, 109250.

(3) Quehenberger, O.; Armando, A. M.; Brown, A. H.; Milne, S. B.; Myers, D. S.; Merrill, A. H.; Bandyopadhyay, S.; Jones, K. N.; Kelly, S.; Shaner, R. L.; Sullards, C. M.; Wang, E.; Murphy, R. C.; Barkley, R. M.; Leiker, T. J.; Raetz, C. R. H.; Guan, Z.; Laird, G. M.; Six, D. A.; Russell, D. W.; McDonald, J. G.; Subramaniam, S.; Fahy, E.; Dennis, E. A. *J. Lipid Res.* **2010**, *51*, 3299−3305.

(4) Huynh, K.; Barlow, C. K.; Jayawardana, K. S.; Weir, J. M.; Mellett, N. A.; Cinel, M.; Magliano, D. J.; Shaw, J. E.; Drew, B. G.; Meikle, P. J. *Cell Chem. Biol.* **2019**, *26*, 71−84.e4.

(5) Quehenberger, O.; Dennis, E. A. *N. Engl. J. Med.* **2011**, *365*, 1812−1823.

(6) Liebisch, G.; Vizcaíno, J. A.; Köfeler, H.; Trötzmüller, M.; Griffiths, W. J.; Schmitz, G.; Spener, F.; Wakelam, M. J. O. *J. Lipid Res.* **2013**, *54*, 1523−1530.

(7) Wei, F.; Lamichhane, S.; Orešič, M.; Hyötyläinen, T. *Trends Anal. Chem.* **2019**, *120*, 115664.

(8) O'Donnell, V. B.; Ekroos, K.; Liebisch, G.; Wakelam, M. *Wiley Interdiscip. Rev.: Syst. Biol. Med.* **2020**, *12*, 1−6.

(9) Wilson, P. W. F.; D'Agostino, R. B.; Levy, D.; Belanger, A. M.; Silbershatz, H.; Kannel, W. B. *Circulation* **1998**, *97*, 1837−1847.

(10) Havulinna, A. S.; Sysi-Aho, M.; Hilvo, M.; Kauhanen, D.; Hurme, R.; Ekroos, K.; Salomaa, V.; Laaksonen, R. *Arterioscler., Thromb., Vasc. Biol.* **2016**, *36*, 2424−2430.

(11) Summers, S. A. *Cell Metab.* **2018**, *27*, 276−280.

(12) Stegemann, C.; Pechlaner, R.; Willeit, P.; Langley, S. R.; Mangino, M.; Mayr, U.; Menni, C.; Moayyeri, A.; Santer, P.; Rungger, G.; Spector, T. D.; Willeit, J.; Kiechl, S.; Mayr, M. *Circulation* **2014**, *129*, 1821−1831.

(13) Fernandez, C.; Sandin, M.; Sampaio, J. L.; Almgren, P.; Narkiewicz, K.; Hoffmann, M.; Hedner, T.; Wahlstrand, B.; Simons, K.; Shevchenko, A.; James, P.; Melander, O. *PLoS One* **2013**, *8*, No. e71846.

(14) Burla, B.; Arita, M.; Arita, M.; Bendt, A. K.; Cazenave-Gassiot, A.; Dennis, E. A.; Ekroos, K.; Han, X.; Ikeda, K.; Liebisch, G.; Lin, M. K.; Loh, T. P.; Meikle, P. J.; Orešič, M.; Quehenberger, O.; Shevchenko, A.; Torta, F.; Wakelam, M. J. O.; Wheelock, C. E.; Wenk, M. R. *J. Lipid Res.* **2018**, *59*, 2001−2017.

(15) Burla, B.; Arita, M.; Arita, M.; Bendt, A. K.; Cazenave-Gassiot, A.; Dennis, E. A.; Ekroos, K.; Han, X.; Ikeda, K.; Liebisch, G.; Lin, M. K.; Loh, T. P.; Meikle, P. J.; Orešič, M.; Quehenberger, O.; Shevchenko, A.; Torta, F.; Wakelam, M. J. O.; Wheelock, C. E.; Wenk, M. R. *J. Lipid Res.* **2018**, *59*, 2001.

(16) Vvedenskaya, O.; Holčapek, M.; Vogeser, M.; Ekroos, K.; Meikle, P. J.; Bendt, A. K. *J. Mass Spectrom. Adv. Clin. Lab* **2022**, *24*, 1−4.

(17) Bowden, J. A.; Heckert, A.; Ulmer, C. Z.; Jones, C. M.; Koelmel, J. P.; Abdullah, L.; Ahonen, L.; Alnouti, Y.; Armando, A. M.; Asara, J. M.; Bamba, T.; Barr, J. R.; Bergquist, J.; Borchers, C. H.; Brandsma, J.; Breitkopf, S. B.; Cajka, T.; Cazenave-Gassiot, A.; Checa, A.; Cinel, M. A.; Colas, R. A.; Cremers, S.; Dennis, E. A.; Evans, J. E.; Fauland, A.; Fiehn, O.; Gardner, M. S.; Garrett, T. J.; Gotlinger, K. H.; Han, J.; Huang, Y.; Neo, A. H.; Hyötyläinen, T.; Izumi, Y.; Jiang, H.; Jiang, H.; Jiang, J.; Kachman, M.; Kiyonami, R.; Klavins, K.; Klose, C.; Köfeler, H. C.; Kolmert, J.; Koal, T.; Koster, G.; Kuklenyik, Z.; Kurland, I. J.; Leadley, M.; Lin, K.; Maddipati, K. R.; McDougall, D.; Meikle, P. J.; Mellett, N. A.; Monnin, C.; Moseley, M. A.; Nandakumar, R.; Oresic, M.; Patterson, R.; Peake, D.; Pierce, J. S.; Post, M.; Postle, A. D.; Pugh, R.; Qiu, Y.; Quehenberger, O.; Ramrup, P.; Rees, J.; Rembiesa, B.; Reynaud, D.; Roth, M. R.; Sales, S.; Schuhmann, K.; Schwartzman, M. L.; Serhan, C. N.; Shevchenko, A.; Somerville, S. E.; St. John-Williams, L.; Surma, M. A.; Takeda, H.; Thakare, R.; Thompson, J. W.; Torta, F.; Triebl, A.; Trötzmüller, M.; Ubhayasekera, S. J. K.; Vuckovic, D.; Weir, J. M.; Welti, R.; Wenk, M. R.; Wheelock, C. E.; Yao, L.; Yuan, M.; Zhao, X. H.; Zhou, S. *J. Lipid Res.* **2017**, *58*, 2275−2288.

(18) Ghorasaini, M.; Mohammed, Y.; Adamski, J.; Bettcher, L.; Bowden, J. A.; Cabruja, M.; Contrepois, K.; Ellenberger, M.; Gajera, B.; Haid, M.; Hornburg, D.; Hunter, C.; Jones, C. M.; Klein, T.; Mayboroda, O.; Mirzaian, M.; Moaddel, R.; Ferrucci, L.; Lovett, J.; Nazir, K.; Pearson, M.; Ubhi, B. K.; Raftery, D.; Riols, F.; Sayers, R.; Sijbrands, E. J. G.; Snyder, M. P.; Su, B.; Velagapudi, V.; Williams, K. J.; de Rijke, Y. B.; Giera, M. *Anal. Chem.* **2021**, *93*, 16369−16378.

(19) Thompson, J. W.; Adams, K. J.; Adamski, J.; Asad, Y.; Borts, D.; Bowden, J. A.; Byram, G.; Dang, V.; Dunn, W. B.; Fernandez, F.; Fiehn, O.; Gaul, D. A.; Hühmer, A. F. R.; Kalli, A.; Koal, T.; Koeniger, S.; Mandal, R.; Meier, F.; Naser, F. J.; O'Neil, D.; Pal, A.; Patti, G. J.; Pham-Tuan, H.; Prehn, C.; Raynaud, F. I.; Shen, T.; Southam, A. D.; St. John-Williams, L.; Sulek, K.; Vasilopoulou, C. G.; Viant, M.; Winder, C. L.; Wishart, D.; Zhang, L.; Zheng, J.; Moseley, M. A. *Anal. Chem.* **2019**, *91*, 14407−14416.

(20) Liebisch, G.; Ahrends, R.; Arita, M.; Arita, M.; Bowden, J. A.; Ejsing, C. S.; Griffiths, W. J.; Holčapek, M.; Köfeler, H.; Mitchell, T. W.; Wenk, M. R.; Ekroos, K.; Lipidomics Standards Initiative Consortium. *Nat. Metab.* **2019**, *1*, 745−747.

(21) Triebl, A.; Burla, B.; Selvalatchmanan, J.; Oh, J.; Tan, S. H.; Chan, M. Y.; Mellet, N. A.; Meikle, P. J.; Torta, F.; Wenk, M. R. *J. Lipid Res.* **2020**, *61*, 105−115.

(22) Lippa, K. A.; Aristizabal-Henao, J. J.; Beger, R. D.; Bowden, J. A.; Broeckling, C. *Metabolomics* **2022**, *18*, 24.

(23) Gouveia, G. J.; Shaver, A. O.; Garcia, B. M.; Morse, A. M.; Andersen, E. C.; Edison, A. S.; McIntyre, L. M. *Anal. Chem.* **2021**, *93*, 9193−9199.

(24) O'Donnell, V. B.; FitzGerald, G. A.; Murphy, R. C.; Liebisch, G.; Dennis, E. A.; Quehenberger, O.; Subramaniam, S.; Wakelam, M. J. O. *Circ.: Genomic Precis. Med.* **2020**, *13*, 737−741.

(25) Köfeler, H. C.; Ahrends, R.; Baker, E. S.; Ekroos, K.; Han, X.; Hoffmann, N.; Holčapek, M.; Wenk, M. R.; Liebisch, G. *J. Lipid Res.* **2021**, *62*, 100138.

(26) Wang, J.; Wang, C.; Han, X. *Anal. Chim. Acta* **2019**, *1061*, 28−41.

(27) Züllig, T.; Trötzmüller, M.; Köfeler, H. C. *Anal. Bioanal. Chem.* **2020**, *412*, 2191−2209.

(28) Huynh, K.; Barlow, C. K.; Jayawardana, K. S.; Weir, J. M.; Mellett, N. A.; Cinel, M.; Magliano, D. J.; Shaw, J. E.; Drew, B. G.; Meikle, P. J. *Cell Chem. Biol.* **2019**, *26*, 71−84.e4.

(29) Han, X.; Gross, R. W. *Mass Spectrom. Rev.* **2005**, *24*, 367−412.

(30) Ejsing, C. S.; Sampaio, J. L.; Surendranath, V.; Duchoslav, E.; Ekroos, K.; Klemm, R. W.; Simons, K.; Shevchenko, A. *Proc. Natl. Acad. Sci. U.S.A.* **2009**, *106*, 2136−2141.

(31) Surma, M. A.; Herzog, R.; Vasilj, A.; Klose, C.; Christinat, N.; Morin-Rivron, D.; Simons, K.; Masoodi, M.; Sampaio, J. L. *Eur. J. Lipid Sci. Technol.* **2015**, *117*, 1540−1549.

(32) Schneider, B. B.; Nazarov, E. G.; Londry, F.; Vouros, P.; Covey, T. R. *Mass Spectrom. Rev.* **2016**, *35*, 687−737.

(33) Contrepois, K.; Mahmoudi, S.; Ubhi, B. K.; Papsdorf, K.; Hornburg, D.; Brunet, A.; Snyder, M. *Sci. Rep.* **2018**, *8*, 17747.

(34) Su, B.; Bettcher, L. F.; Hsieh, W.-Y.; Hornburg, D.; Pearson, M. J.; Blomberg, N.; Giera, M.; Snyder, M. P.; Raftery, D.; Bensinger, S. J.; Williams, K. J. *J. Am. Soc. Mass Spectrom.* **2021**, *32*, 2655−2663.

(35) Han, X.; Yang, K.; Gross, R. W. *Mass Spectrom. Rev.* **2012**, *31*, 134−178.

(36) Han, X.; Gross, R. W. *J. Lipid Res.* **2022**, *63*, 100164.

(37) Chollet, C.; Boutet-Mercey, S.; Laboureur, L.; Rincon, C.; Méjean, M.; Jouhet, J.; Fenaille, F.; Colsch, B.; Touboul, D. *J. Mass Spectrom.* **2019**, *54*, 791−801.

(38) Wolrab, D.; Chocholoušková, M.; Jirásko, R.; Peterka, O.; Holčapek, M. *Anal. Bioanal. Chem.* **2020**, *412*, 2375−2388.

(39) Lange, M.; Fedorova, M. *Anal. Bioanal. Chem.* **2020**, *412*, 3573−3584.

(40) Cífková, E.; Holčapek, M.; Lísa, M.; Ovčačíková, M.; Lyčka, A.; Lynen, F.; Sandra, P. *Anal. Chem.* **2012**, *84*, 10064−10070.

(41) Cífková, E.; Hájek, R.; Lísa, M.; Holčapek, M. *J. Chromatogr. A* **2016**, *1439*, 65−73.

(42) Schoeny, H.; Rampler, E.; El Abiead, Y.; Hildebrand, F.; Zach, O.; Hermann, G.; Koellensperger, G. *Analyst* **2021**, *146*, 2591−2599.

(43) Munjoma, N.; Isaac, G.; Muazzam, A.; Cexus, O.; Azhar, F.; Pandha, H.; Whetton, A. D.; Townsend, P. A.; Wilson, I. D.; Gethings, L. A.; Plumb, R. S. *J. Proteome Res.* **2022**, *21*, 2596−2608.

(44) Wang, M.; Wang, C.; Han, X. *Mass Spectrom. Rev.* **2017**, *36*, 693−714.

(45) Carrard, J.; Gallart-Ayala, H.; Infanger, D.; Teav, T.; Wagner, J.; Knaier, R.; Colledge, F.; Streese, L.; Königstein, K.; Hinrichs, T.; Hanssen, H.; Ivanisevic, J.; Schmidt-Trucksäss, A. *Metabolites* **2021**, *11*, 287.

(46) Medina, J.; van der Velpen, V.; Teav, T.; Guitton, Y.; Gallart-Ayala, H.; Ivanisevic, J. *Metabolites* **2020**, *10*, 495.

(47) Gao, L.; Ji, S.; Burla, B.; Wenk, M. R.; Torta, F.; Cazenave-Gassiot, A. *Anal. Chem.* **2021**, *93*, 3163−3171.

(48) Sarafian, M. H.; Gaudin, M.; Lewis, M. R.; Martin, F. P.; Holmes, E.; Nicholson, J. K.; Dumas, M. E. *Anal. Chem.* **2014**, *86*, 5766−5774.

(49) Meister, I.; Zhang, P.; Sinha, A.; Sköld, C. M.; Wheelock, Å. M.; Izumi, T.; Chaleckis, R.; Wheelock, C. E. *Anal. Chem.* **2021**, *93*, 5248−5258.

(50) Zhang, Y.; Xie, Y.; Lv, W.; Hu, C.; Xu, T.; Liu, X.; Zhang, R.; Xu, G.; Xia, Y.; Zhao, X. *J. Chromatogr. A* **2021**, *1651*, 462271.

(51) Hsu, F. F.; Turk, J. *J. Chromatogr. B: Anal. Technol. Biomed. Life Sci.* **2009**, *877*, 2673−2695.

(52) Cao, Z.; Schmitt, T. C.; Varma, V.; Sloper, D.; Beger, R. D.; Sun, J. *J. Proteome Res.* **2020**, *19*, 2742−2749.

(53) Loef, M.; von Hegedus, J. H.; Ghorasaini, M.; Kroon, F. P. B.; Giera, M.; Ioan-Facsinay, A.; Kloppenburg, M. *Metabolites* **2021**, *11*, 26.

(54) Yang, K.; Han, X. *Metabolites* **2011**, *1*, 21−40.

(55) Visconti, G.; Olesti, E.; González-Ruiz, V.; Glauser, G.; Tonoli, D.; Lescuyer, P.; Vuilleumier, N.; Rudaz, S. *Talanta* **2022**, *240*, 123149.

(56) Huynh, K.; Mellett, N. A.; Duong, T.; Nguyen, A.; Meikle, T. G.; Giles, C.; Meikle, P. J.; Sartain, M. A Comprehensive, Curated, High-Throughput Method for the Detailed Analysis of the Plasma Lipidome. *Agil. Appl. Note* **2021**.

(57) Triebl, A.; Burla, B.; Selvalatchmanan, J.; Oh, J.; Tan, S. H.; Chan, M. Y.; Mellet, N. A.; Meikle, P. J.; Torta, F.; Wenk, M. R. *J. Lipid Res.* **2020**, *61*, 105−115.

(58) Mittelstrass, K.; Ried, J. S.; Yu, Z.; Krumsiek, J.; Gieger, C.; Prehn, C.; Roemisch-Margl, W.; Polonikov, A.; Peters, A.; Theis, F. J.; Meitinger, T.; Kronenberg, F.; Weidinger, S.; Wichmann, H. E.; Suhre, K.; Wang-Sattler, R.; Adamski, J.; Illig, T. *PLoS Genet.* **2011**, *7*, No. e1002215.

(59) Beyene, H. B.; Olshansky, G.; Smith, A. A. T.; Giles, C.; Huynh, K.; Cinel, M.; Mellett, N. A.; Cadby, G.; Hung, J.; Hui, J.; Beilby, J.; Watts, G. F.; Shaw, J. S.; Moses, E. K.; Magliano, D. J.; Meikle, P. J. *PLoS Biol.* **2020**, *18*, No. e3000870.

(60) Krumsiek, J.; Mittelstrass, K.; Do, K. T.; Stückler, F.; Ried, J.; Adamski, J.; Peters, A.; Illig, T.; Kronenberg, F.; Friedrich, N.; Nauck, M.; Pietzner, M.; Mook-Kanamori, D. O.; Suhre, K.; Gieger, C.; Grallert, H.; Theis, F. J.; Kastenmüller, G. *Metabolomics* **2015**, *11*, 1815−1833.

(61) Slade, E.; Irvin, M. R.; Xie, K.; Arnett, D. K.; Claas, S. A.; Kind, T.; Fardo, D. W.; Graf, G. A. *Lipids Health Dis.* **2021**, *20*, 1−12.

(62) Trabado, S.; Al-Salameh, A.; Croixmarie, V.; Masson, P.; Corruble, E.; Fève, B.; Colle, R.; Ripoll, L.; Walther, B.; Boursier-Neyret, C.; Werner, E.; Becquemont, L.; Chanson, P. *PLoS One* **2017**, *12*, No. e0173615.

(63) Ishikawa, M.; Maekawa, K.; Saito, K.; Senoo, Y.; Urata, M.; Murayama, M.; Tajima, Y.; Kumagai, Y.; Saito, Y. *PLoS One* **2014**, *9*, No. e91806.

(64) Wong, M. W. K.; Braidy, N.; Pickford, R.; Vafaee, F.; Crawford, J.; Muenchhoff, J.; Schofield, P.; Attia, J.; Brodaty, H.; Sachdev, P.; Poljak, A. *PLoS One* **2019**, *14*, No. e0214141.

(65) Sales, S.; Graessler, J.; Ciucci, S.; Al-Atrib, R.; Vihervaara, T.; Schuhmann, K.; Kauhanen, D.; Sysi-Aho, M.; Bornstein, S. R.; Bickle, M.; Cannistraci, C. V.; Ekroos, K.; Shevchenko, A. *Sci. Rep.* **2016**, *6*, 27710.

(66) Gonzalez-Covarrubias, V.; Beekman, M.; Uh, H. W.; Dane, A.; Troost, J.; Paliukhovich, I.; van der Kloet, F. M.; Houwing-Duistermaat, J.; Vreeken, R. J.; Hankemeier, T.; Slagboom, E. P. *Aging Cell* **2013**, *12*, 426−434.

(67) Nikkilä, J.; Sysi-Aho, M.; Ermolov, A.; Seppänen-Laakso, T.; Simell, O.; Kaski, S.; Orešič, M. *Mol. Syst. Biol.* **2008**, *4*, 197.

(68) Merrill, A. H.; Wang, E.; Innis, W. S. A.; Mullins, R. *Lipids* **1985**, *20*, 252−254.

(69) McClelland, D. R.; Bourdelat-Parksi, B.; Salata, K.; Francis, G. L. *Endocrinol. Metab.* **1997**, *4*, 19−24.

(70) Lucki, N. C.; Sewer, M. B. Multiple Roles for Sphingolipids in Steroid Hormone Biosynthesis. In *Lipids in Health and Disease*; Springer Netherlands: Dordrecht, 2012; Vol. 78, pp 387−412.

(71) Draper, C. F.; Duisters, K.; Weger, B.; Chakrabarti, A.; Harms, A. C.; Brennan, L.; Hankemeier, T.; Goulet, L.; Konz, T.; Martin, F. P.; Moco, S.; van der Greef, J. *Sci. Rep.* **2018**, *8*, 14568.

(72) Lucki, N. C.; Sewer, M. B. *Steroids* **2010**, *75*, 390−399.

(73) Karsai, G.; Lone, M.; Kutalik, Z.; Brenna, J.; Li, H.; Pan, D.; von Eckardstein, A.; Hornemann, X. *J. Biol. Chem.* **2020**, *295*, 1889−1897.

(74) Muilwijk, M.; Callender, N.; Goorden, S.; Vaz, F. M.; van Valkengoed, I. G. M. *Biol. Sex Differ.* **2021**, *12*, 1−14.

(75) Li, Z.; Vance, D. E. *J. Lipid Res.* **2008**, *49*, 1187−1194.

(76) Emokpae, M. A.; Uwumarongie, O. H.; Osadolor, H. B. *Indian J. Clin. Biochem.* **2011**, *26*, 57−61.

(77) Brilakis, E. S.; Khera, A.; McGuire, D. K.; See, R.; Banerjee, S.; Murphy, S. A.; de Lemos, J. A. *Atherosclerosis* **2008**, *199*, 110−115.

(78) Dean, J. M.; Lodhi, I. J. *Protein Cell* **2018**, *9*, 196−206.

(79) Watschinger, K.; Werner, E. R. *IUBMB Life* **2013**, *65*, 366−372.

(80) Sales, S.; Graessler, J.; Ciucci, S.; Al-Atrib, R.; Vihervaara, T.; Schuhmann, K.; Kauhanen, D.; Sysi-Aho, M.; Bornstein, S. R.; Bickle,

M.; Cannistraci, C. V.; Ekroos, K.; Shevchenko, A. *Sci. Rep.* **2016**, *6*, 27710.

📖 Recommended by ACS

Rapid Multi-Omics Sample Preparation for Mass Spectrometry

Laura K. Muehlbauer, Joshua J. Coon, *et al.*

JANUARY 02, 2023
ANALYTICAL CHEMISTRY READ 🗗

Differential Kendrick's Plots as an Innovative Tool for Lipidomics in Complex Samples: Comparison of Liquid Chromatography and Infusion-Based Methods to Sample...

Justine Hustin, Edwin De Pauw, *et al.*

NOVEMBER 15, 2022
JOURNAL OF THE AMERICAN SOCIETY FOR MASS SPECTROMETRY READ 🗗

High Throughput LC-MS Platform for Large Scale Screening of Bioactive Polar Lipids in Human Plasma and Serum

Nyasha Munjoma, Robert S. Plumb, *et al.*

OCTOBER 20, 2022
JOURNAL OF PROTEOME RESEARCH READ 🗗

Development of a Miniature Mass Spectrometry System for Point-of-Care Analysis of Lipid Isomers Based on Ozone-Induced Dissociation

Xinwei Liu, Zheng Ouyang, *et al.*

SEPTEMBER 29, 2022
ANALYTICAL CHEMISTRY READ 🗗

Get More Suggestions >